Desalination and Water Treatment
www.deswater.com
doi: 10.1080/19443994.2013.813102

52 (2014) 5563–5574
August

Taylor & Francis
Taylor & Francis Group

Adsorption of malachite green from aqueous solutions onto lotus leaf: equilibrium, kinetic, and thermodynamic studies

Xiuli Han*, Jinyi Yuan, Xiaojian Ma

School of Chemical Engineering and Energy, Zhengzhou University, Kexue Road 100#, Zhengzhou,
Henan 450001, P.R. China
Tel. +86 371 67780093; Fax: +86 371 63887311; email: xlhan@zzu.edu.cn

Received 19 January 2012; Accepted 20 May 2013

ABSTRACT

The low-cost and highly efficient adsorbents have been investigated to remove dyes from aqueous solution. In this study, lotus leaf was used as a biosorbent for the removal of malachite green (MG) from aqueous solutions. The batch experiments used to investigate the effect of experimental parameters such as contact time, adsorbent dose, initial MG concentration, solution pH, salt ionic strength, and temperature. The Langmuir, Freundlich, Koble–Corrigan and Redlich–Peterson isotherm models were considered to evaluate the adsorption behavior. The adsorption behavior was best described by the Koble–Corrigan, Redlich–Peterson and Langmuir isotherms. The maximum monolayer adsorption capacities of lotus leaf for MG were 105.9, 113.8, and 125.3 mg g^{-1} at 296, 306, and 316 K, respectively. The adsorption process followed the pseudo-second-order rate equation which suggested that the adsorption may be a chemisorption process. Thermodynamic parameters of ΔG, ΔH, and ΔS indicated the adsorption process was spontaneous and endothermic. A large number of carbonyl and hydroxyl groups were found on the surface of the lotus leaf through FTIR analysis. The present study suggested that lotus leaf has high potential to be used as low-cost adsorbent for MG removal.

Keywords: Adsorption; Malachite green; Lotus leaf; Isotherm; Kinetics; Thermodynamics

1. Introduction

Dyestuffs are considered to be color organic compounds, which are widely used in many industries, such as the textiles, cosmetics, leather, food, paper and so on. Around the world, there are about 700,000 tons and 10,000 types of different commercial dyes and pigments are being produced annually [1]. It is reported that 10–15% of used dyes enter the environment through wastes [2]. The discharge of the colored effluent will pose a threat to humans and the environment, because dyes are toxic, it can affect man through the food chain and the photosynthesis of aquatic plants. In addition, they also impact the transmission of light and upset the biological metabolism processes which cause the destruction of aquatic present in ecosystem [3]. So the techniques of removal of harmful dyes from colored wastewater attract more and more attention of many scientists.

The numerous techniques of dye removal have been reported by many researchers, and several physical, chemical, and biological methods have been

---

*Corresponding author.

1944-3994/1944-3986

used, such as filtration, membrane filtration, precipitation, ion exchange, flocculation, electrochemical and so on [4]. However, these methods suffered from one or more limitation and not always effective and economical. The adsorption technique is the simplest and most efficient method. The efficiency of the adsorption process mainly rests with the economical and removal capacity of adsorbents. As we all known that activated carbon has been common used as an adsorbent but its high cost poses an economical problem [5]. Nowadays, non-conventional low-cost adsorbents such as agricultural waste materials, natural materials, bioadsorbents attract more attention for the dye removal [6]. Many low-cost adsorbents have been studied by home or aboard researchers, such as corynebacterium glutamicum [7], potato peel [8], bentonite [9], cashew nut shell [10], olive pomace [11], chitin, rice husk, wood, fly ash and so on [12].

MG is crystalline, belongs to triphenylmethane dyes. MG is very dangerous and has highly cytotoxic property against mammalian cells and also plays a pivotal role as a liver tumor-enhancing agent. Various studies have been made to remove MG from the wastewater. A number of materials including activated carbon [13,14], neem sawdust [15], rattan sawdust [16], clayey soil [17], and mango seed husks [18] have been shown to be successful adsorbent materials for the removal of MG from aqueous solutions.

Lotus is commonly grown in subtropical and temperate regions of china, lotus leaf as agricultural and easily available waste contains abundant floristic fiber, protein, and some functional groups, so lotus leaf can be used as a low-cost adsorbent for the removal of dye. The objective of this investigation is to study the removal of MG from aqueous solution by lotus leaf, investigated relevant parameters which may affect the adsorption process.

2. Materials and methods

2.1. Preparation of adsorbents

Lotus leaf used in this research was purchased from farmland in Jiangsu Province of China. The collected biomaterial was thoroughly washed with tap water to remove the dust and other impurities then rinsed with distilled water. Leaves were firstly dried at room temperature and then in hot air oven at 65℃ for 6 h. The dried leaves were grinded, sieved by standard sieves. Resulting lotus leaves powder were kept in a glass bottle for use in adsorption experiments. The particle size of leaves used in the study was 20–40 mesh.

2.2. Preparation of dye solution

The dye, MG hydrochloride [C.I. no: 42000, $C_{23}H_{26}N_2Cl$, FW = 364.92] was supplied by Tianjin Chemical Equipment Company. A stock solution of MG was prepared by dissolving an appropriate amount of dye in distilled water. Experimental solutions of the desired concentration were obtained by successive dilutions.

2.3. Adsorption experiments

The adsorption experiments were carried out in a batch process by using aqueous solutions of malachite green. The effect of different experimental conditions such as pH, biosorbent dosage, initial dye concentration, contact time, ionic strength, and temperature were studied. In each adsorption experiment, the preweighed amount of adsorbents were added to 50-mL conical flasks containing 10 mL of known initial concentration and initial pH value of MG solution, and then, the mixture was agitated at 100 rpm on a water bath shaker for a given length of time at a constant temperature. After shaking, the biosorbent/dye mixtures were separated from solution by centrifugation, and the supernatants were analyzed by a WFZ UV-2102PC Spectrophotometer at characteristic wavelength ($\lambda_{\max} = 618\,\text{nm}$) in order to determine the residual concentration. The pH values of the solutions ranging from 2 to 10, the initial pH was previous adjusted with $0.1\,\text{mol}\,\text{L}^{-1}$ HCl and $0.1\,\text{mol}\,\text{L}^{-1}$ NaOH using a pH meter. The effect of salt ionic strength was discussed over the NaCl or $CaCl_2$ concentration range from 0.01 to $0.2\,\text{mol}\,\text{L}^{-1}$. For adsorption isotherm, dye solutions of different concentrations ($30\text{–}200\,\text{mg}\,\text{L}^{-1}$) were shaken with the known amount of adsorbent at 296, 306, 316 K till reached the equilibrium. The kinetic experiments were carried out by analyzing adsorptive uptake of the dye of known concentrations from 30 to $200\,\text{mg}\,\text{L}^{-1}$ at different time intervals.

The amount of MG adsorbed on per gram lotus leaf and the percentage removal of MG solution were calculated by Eqs. (1) and (2), respectively:

$$q_e = \frac{V(C_0 - C_e)}{m} \tag{1}$$

$$R\% = \frac{C_0 - C_e}{C_0} \times 100\% \tag{2}$$

where q_e ($\text{mg}\,\text{g}^{-1}$) is the amount of dye adsorbed on per gram adsorbent at the time of equilibrium, C_0 and C_e ($\text{mg}\,\text{L}^{-1}$) are the initial and equilibrium concentrations of dye, respectively, V(L) is the volume of solution and m(g) is the mass of dry adsorbent, $R\%$ is the percentage removal of MG.

3. Adsorption models

3.1. Adsorption equilibrium isotherm models

The adsorption isotherms are important for the description of adsorption system. Isotherm expresses the relation between equilibrium concentration, temperature of the adsorbate in the solid phase and in the liquid phase. In this research, Langmuir, Freundlich, Koble–Corrigan and Redlich–Peterson isotherms were applied to the equilibrium data of adsorption.

The Langmuir model assumes uniform energies of adsorption onto the surface without transmigration of adsorbate in the plane of the surface [19]. The nonlinear equation may be written as follows:

$$q_e = \frac{q_m K_L C_e}{1 + K_L C_e} \tag{3}$$

where q_m (mg g^{-1}) is the monolayer biosorption capacity per weight of adsorbent, q_e (mg g^{-1}) is the adsorption capacity per unit weight of adsorbent at equilibrium, K_L (L mg^{-1}) is the Langmuir constant, C_e (mg L^{-1}) is the equilibrium concentration of the dye solution.

The Freundich isotherm model suggests that adsorption enthalpy exponentially decreases with the increasing degree of site occupation [11]. The nonlinear equation is expressed as:

$$q_e = K_F C_e^{1/n} \tag{4}$$

where K_F (mg g^{-1}(L mg^{-1})$^{1/n}$) and $1/n$ are Freundlich constants, C_e (mg L^{-1}) is the equilibrium concentration of the solution, q_e (mg g^{-1}) is the adsorption capacity per unit weight of adsorbent at equilibrium.

Koble–Corrigan model [12] is the combination of Langmuir and Freundlich isotherm type models. The following equation represents this model:

$$q_e = \frac{A_K C_e^M}{1 + B_K C_e^M} \tag{5}$$

where A_K, B_K, and M are the Koble–Corrigan parameters.

Redlich–Peterson model [20] is an empirical equation which has been proposed to improve the fit by Langmuir and Freunlich models. The non-linear equilibrium equation:

$$q_e = \frac{A C_e}{1 + B C_e^g} \tag{6}$$

where A, B, and g are Redlich–Peterson parameters, g must fluctuate between 0 and 1.

3.2. Adsorption kinetic models

In order to investigate the controlling mechanism of adsorption process such as diffusion control, chemical reaction and mass transfer. The commonly used kinetic models are the pseudo-first-order model, the pseudo-second-order model and intraparticle diffusion model.

3.2.1. The pseudo-first-order model

The pseudo-first-order equation is the earliest known equation describing the adsorption rate. The equation can be expresses as follows [21]:

$$\frac{dq_t}{d_t} = k_1(q_e - q_t) \tag{7}$$

Through integration and applying boundary conditions $q_t = 0$ at $t = 0$; the equation becomes:

$$q_t = q_e(1 - e^{-k_1 t}) \tag{8}$$

where q_e (mg g^{-1}) and q_t (mg g^{-1}) are the adsorption capacity per unit weight of adsorbent at equilibrium and at time t, respectively, k_1 (min^{-1}) is the rate constant of the pseudo-first order sorption.

3.2.2. The pseudo-second-order model

The pseudo-second-order model used in this study is based on the sorption capacity of the solid phase. The equation of the model is generally given as follow [22]:

$$\frac{dq_t}{dt} = k_2(q_e - q_t)^2 \tag{9}$$

After integrating the equation for the boundary conditions $q_t = 0$ at $t = 0$, the nonlinear form of the equation becomes:

$$q_t = \frac{k_2 q_e^2 t}{1 + k_2 q_e t} \tag{10}$$

where k_2 (g mg^{-1} min^{-1}) is the rate constant of pseudo-second order adsorption.

3.2.3. The intraparticle diffusion model

The intraparticle diffusion model is applied to explain the mechanisms and rate-controlling steps of the adsorption kinetics, the adsorption data can be presented by the equation as follows [23,24]:

$$q_t = k_t t^{0.5} + C \tag{11}$$

where k_t (mg g^{-1} min$^{-1/2}$) is the intraparticle diffusion rate constant, C (mg g^{-1}) is a constant.

4. Results and discussion

4.1. Characteristic of lotus leaf

Figs. 1 and 2 show the scanning electron micrographs (JEOL 6335F-SEM, Japan) of adsorbent before and after dye adsorption. The SEM used to characterize the surface morphology and fundamental physical properties of the adsorbent. It is useful for determining the particle shape, porosity and appropriate size distribution of the adsorbent. It can be seen from Fig. 1 that there are a large number of pores. Fig. 2 shows clearly very distinguished dark which can be taken as a sign for effective adsorption of dye molecules in the cavities and pores of this adsorbent.

The Fourier transform infrared spectrometer (PE-1710, USA) is an important technique to understand the chemical structure of the adsorbent. The FTIR spectrum of lotus leaf and dye loaded-lotus leaf is shown in Fig. 3. From Fig. 3, it can be seen that the characteristic function groups of lotus leaf has changed after adsorption. Fig. 3(a) displays some adsorption peaks which indicate the structure of the adsorbent. There is a strong peak at 3,424 cm^{-1} representing the stretch vibration of bonded hydroxyl groups on the surface of material. The peak at 2,922 cm^{-1} indicates the asymmetrical stretch vibration of $-CH_3$. The band observes at about 2852 cm^{-1} could be attributed to the symmetrical stretch vibration of $-CH_2$. The appearance of peak at 1622 cm^{-1} is the characteristic of stretch vibration of $C=O$ from carboxylic acid with intermolecular hydrogen bond. The peaks near around 1055 cm^{-1} can be due to the –OH bending and C-O-C bending in lignin structure of the material. These groups such as carbonyl and hydroxyl groups may function as proton donors, and hence, deprotonated hydroxyl and carboxyl groups may be involved in coordination with positive dye ions. Dissolved MG ions are positively charged and will undergo attraction on approaching the anionic lotus leaf structure. The adsorption of MG ion on lotus leaf may likely be due to the electrostatic attraction between these groups and the cationic of MG. On this basis, it is expected that an MG ion will have a strong sorption affinity by lotus leaf.

It is observed from Fig. 3 that after adsorbing MG on lotus leaf there were changes in intensity and slight shift in position of the peaks, which suggested that there was a binding process taking place on the surface of the adsorbent. A new peak at 1,585 cm^{-1} appeared after lotus leaf was loaded with MG, which is assigned to aromatic ring of MG [25]. These observations confirm the interaction between MG and the

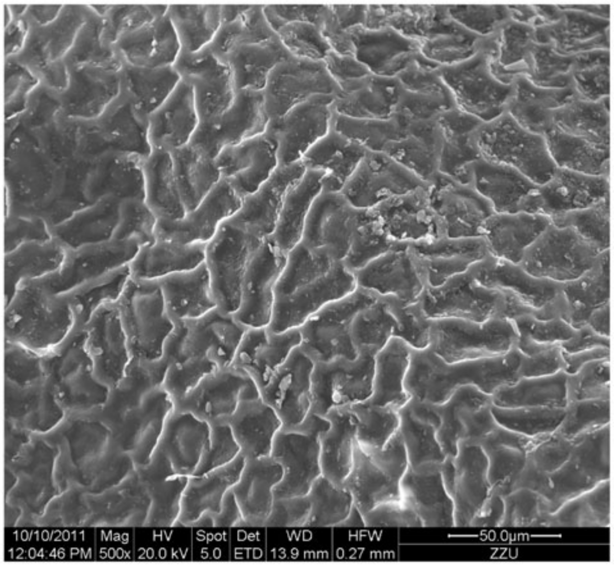

Fig. 1. SEM micrograph for lotus leaf.

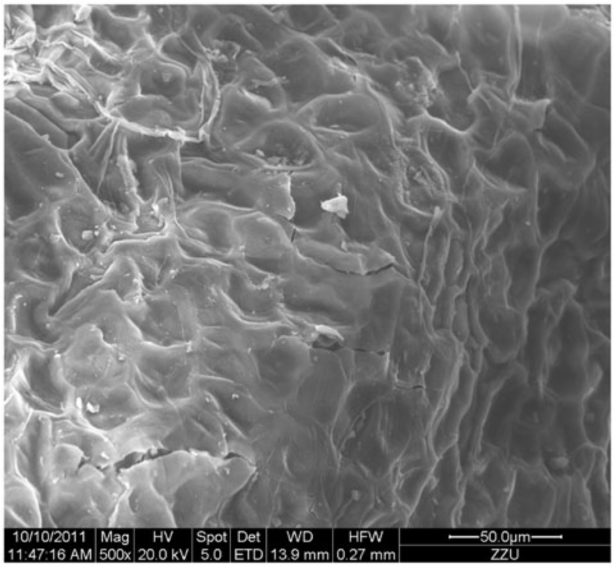

Fig. 2. SEM micrograph for lotus leaf after adsorption of MG.

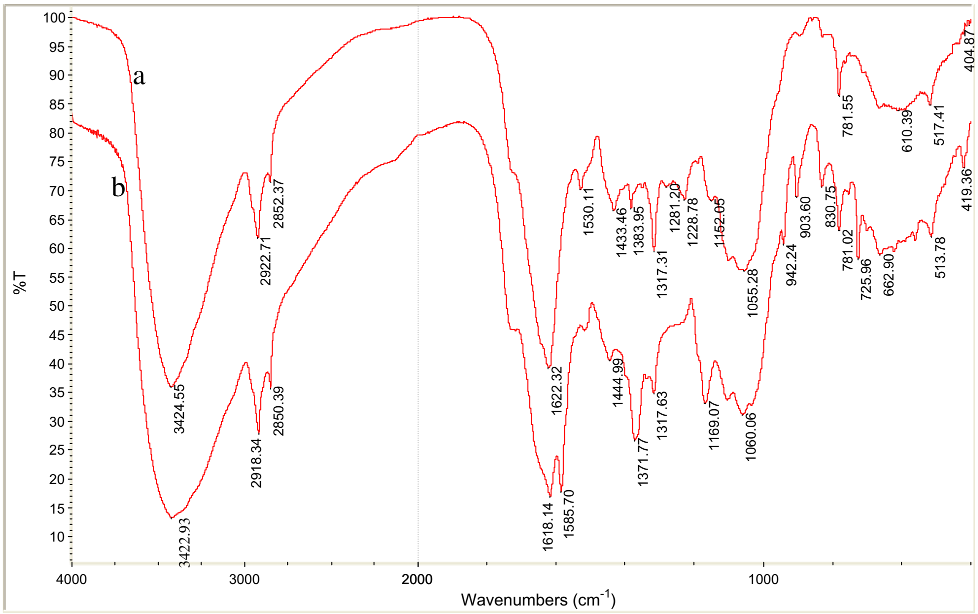

Fig. 3. FTIR spectra of lotus leaf (a) and lotus leaf adsorbed MG (b).

lotus leaf. From the result of the FTIR spectra analysis, it was clear that lotus leaf possessed several functional groups such as carbonyl and hydroxyl groups and these groups could be the potential active sites for the adsorption of dye.

4.2. Influence of contact time

Contact time is an essential factor influencing adsorption of MG on lotus leaf. It can be well-known that the removal efficiency of dye by biosorbents increases with increasing contact time. Fig. 4 shows the effect of contact time on the adsorption of MG by dried leaves. It is showed rapid adsorption of dyes in the first 150 min and, thereafter, the adsorption rate decreased gradually and the adsorption reached equilibrium in about 400 min. Further increase in contact time did not enhance the adsorption. The initial high adsorption rate may be explained by a large number of active vacant sites on the surface of lotus leaf are available for adsorption. After lapse of some time, the adsorption rate becomes slower and its attribute to the decreased availability of binding sites on the surface of biosorbents.

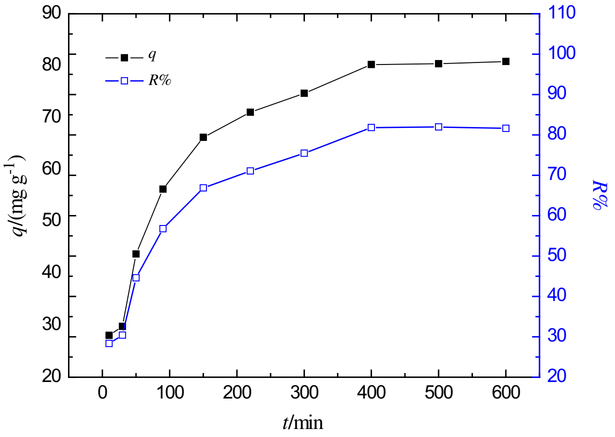

Fig. 4. Effect of contact time on the adsorption of MG ($C_0 = 100\,\mathrm{mg\,L^{-1}}$; adsorbent concentration = $1\,\mathrm{g\,L^{-1}}$; initial pH 4.5; $T = 293\,\mathrm{K}$).

Adsorption equilibrium was nearly established in virtue of the repulsive forces between the dye molecules on the solid surface and the bulk phase [26]. The contact time was fixed at 420 min for the rest of the batch experiments to make sure that equilibration was reached.

4.3. Influence of initial pH

The pH of dye solution has significant effect on the biosorption efficiency of MG through present studies. Fig. 5 shows the effect of pH on MG removal by lotus leaf. This figure indicates that the biosorption capacity of biomass for MG increased from 48 to 84% with increase in pH from 2 to 4. The removal then did no significant variations in the pH range from 4 to 9. It can be seen that the dye biosorption was lower at pH 2 and reached a maximum level at pH range from 4 to 8. Similar trends of pH were reported for the adsorption of MG onto Pyracantha coccinea berries and Macrophyte Alligator Weed [27,28]. The low

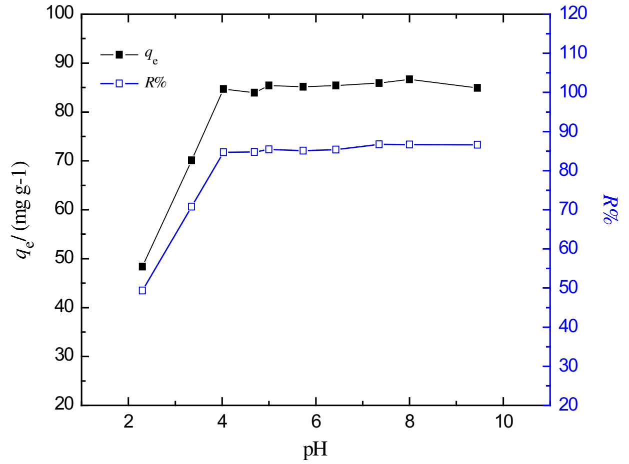

Fig. 5. Effect of pH on the adsorption of MG ($C_0 = 100\,\mathrm{mg\,L^{-1}}$; adsorbent concentration = $1\,\mathrm{g\,L^{-1}}$; $t = 420\,\mathrm{min}$; $T = 293\,\mathrm{K}$).

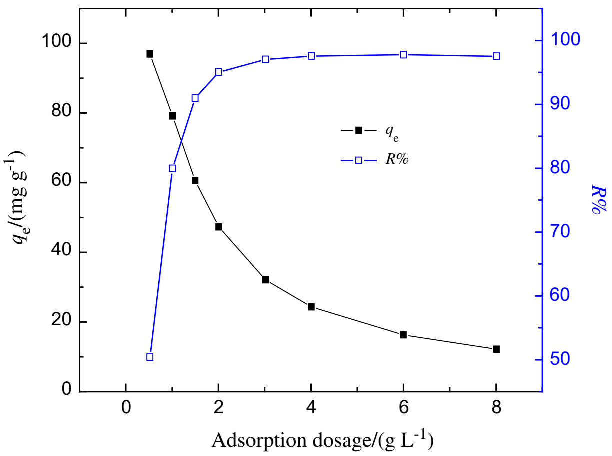

Fig. 6. Effect of adsorbent dose on the adsorption of MG ($C_0 = 100\,\mathrm{mg\,L^{-1}}$; Initial pH 4.5; $t = 420\,\mathrm{min}$; $T = 293\,\mathrm{K}$).

biosorption of MG under low pH is probably explained by the competition of excess H^+ ions with the dye cation MG^+ for the adsorption sites. On the other hand, as the solution pH increased, the adsorbent surface became predominantly negatively charged, a strong electrostatic attraction appears between the cationic dye molecule and the negatively charged leaf surface. However, because of the slightly change of adsorption capacity at the pH range of 4–9, the mechanism for dye adsorption is not only electrostatic mechanism but also have chemical reaction mechanism. The original pH of MG was about 4.5, so the research of other experiments were all use the initial pH of the dye solution.

4.4. Influence of adsorbent dose

Adsorbent dose is an important parameter influencing adsorption processes. Fig. 6 shows the adsorption removal of MG and the value of q_e at different adsorbent dose. The adsorbent dosages varied from 0.5–8 $\mathrm{g\,L^{-1}}$ using an MG concentration of 100 $\mathrm{mg\,L^{-1}}$ and the contact time of 420 min. When adsorbent dosage was increased, it can be seen that the $R\%$ increased from 50.3 to 97.5%, but the adsorption capacity (q_e) presented the opposite trend. The MG removal curve reaches equilibrium when the dosage of the adsorbent is more than 2 $\mathrm{g\,L^{-1}}$. The $R\%$ up to certain limit can be attributed to an increase in the adsorptive surface area and the availability of more active binding adsorption sites [17]. Lower biosorption capacity of MG at a higher adsorbent dose due to the adsorption competition among adsorbent and the split in the concentration gradient [29]. As the adsorbent dose was 1 $\mathrm{g\,L^{-1}}$, the $R\%$ and q_e were 79.95% and 79.15 $\mathrm{mg\,g^{-1}}$, respectively. Considering both biosorption capacity and the removal percentage, the biosorption amount of 1 $\mathrm{g\,L^{-1}}$ was chosen for all further batch experiments.

4.5. Influence of salt ionic concentration

The wastewater from textile-manufacturing or dye-producing industries contains various high salt concentration which may significantly affect the performance of the adsorption process. Fig. 7 shows the effect of ionic concentration on the adsorption of MG onto lotus leaf at 0–0.2 $\mathrm{mol\,L^{-1}}$ NaCl and $CaCl_2$ concentration at 296 K. From the plot, it was observed that the q_e and $R\%$ decreased with increased ionic concentration. The value of q_e decreased from 80.1 to

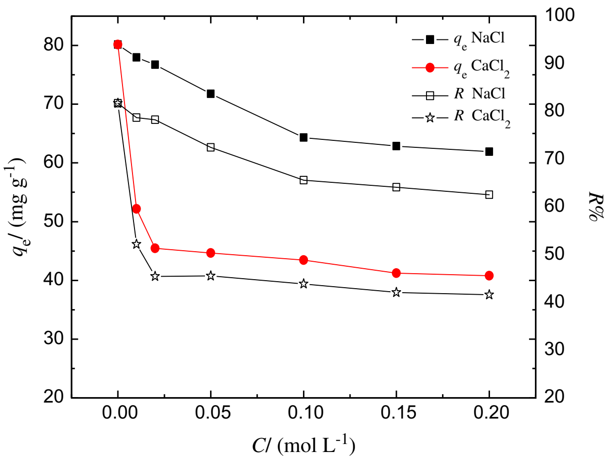

Fig. 7. Effect of salt ionic concentration on the adsorption of MG ($C_0 = 100\,\mathrm{mg\,L^{-1}}$; adsorbent concentration = $1\,\mathrm{g\,L^{-1}}$; $t = 420\,\mathrm{min}$; $T = 293\,\mathrm{K}$).

61.9 mg g^{-1}, 80.1 to 40.7 mg g^{-1} for NaCl and $CaCl_2$, the *R*% decreased from 81.7 to 62.5%, 81.7 to 41.5% for NaCl and $CaCl_2$, respectively, as the concentration of ionic increased from 0 to 0.2 mol L^{-1}. This behavior may be attributed to competition of Na^+ and Ca^{2+} with positively charged dye molecules for the same binding sites on the adsorbent surface in the MG solution. Similar effect was reported [30]. From Fig. 7, the effect of $CaCl_2$ on the adsorption of MG was stronger than NaCl. It may be due to unit mol divalent Ca^{2+} contributed more positive charge than unit mol univalent Na^+.

4.6. Influence of initial dye concentration

It is well established that temperature and initial dye concentration have great effect on the adsorption process. Fig. 8 shows the effect of varying dye concentrations on adsorption of MG onto lotus leaf at different temperatures 296, 306 and 316 K. It is evident from the figure that q_e increased with the increase in initial dye concentration. The initial concentration provided a powerful driving force to overcome the resistance to the mass transfer of MG between the aqueous and solid phases [31]. As shown in Fig. 8, the adsorption capacity increased when the temperature of dye solutions increases from 296 to 316 K, which indicates that the adsorption process in this system is endothermic and chemisorption in nature. The fact is that the adsorption process in favor of high temperature may be due to the increased penetration of dyes inside micropores at high temperature or the increased surface activity and kinetic energy of the solute molecules [32].

4.7. Equilibrium modeling

In order to evaluate different isotherms and their ability to correlate with experimental results, the non-linear plot of q_e against C_e at three temperatures for each isotherm model are shown in Fig. 9. The parameters of different modeling from non-linear method are listed in Table 1. For the Langmuir model, the maximum monolayer adsorption of MG onto lotus leaf is 125.3 mg g^{-1} at the temperature of 316 K. The values of q_m and K_L increased with the increasing temperature, indicating that increasing temperature induced a higher maximum adsorption capacity.

K_F and n are all Freundlich constants, K_F is related to the adsorption capacity of the sorbent and n gives a measure of favorability of adsorption. The value of $1/n$ less than 1 represents favorable adsorption condition. The values of K_F and n at different temperature showed that the adsorption behavior was carried out easily. The Koble–Corrigan isotherm also agree very well with the experimental data of MG dye ($R^2 > 0.985$), indicating that the Koble–Corrigan model is suitable for describing the adsorption process. The Redlich–Peterson isotherm constants are A and B, the exponent g reflecting the heterogeneity of the sorbent, the value of g is between 0 to 1. The constant g can characterize the isotherm as: if $g = 0$, the Freundlich will be the desirable isotherm, while if $g = 1$, the Langmuir will be the preferable isotherm. It can be seen from Table 1, the value of g tends to 1, which indicates that the isotherms are propinquity Langmuir form. According to the correlation coefficients, R-P, K-C and Langmuir isotherms could better represent the

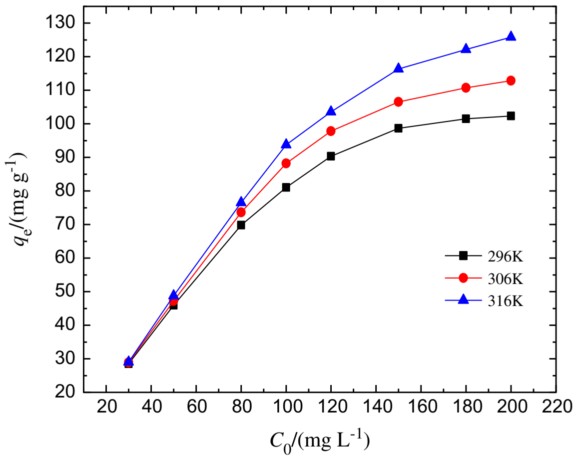

Fig. 8. Effect of initial dye concentration on the adsorption of MG ($T = 296$, 306, and 316 K; adsorbent concentration = 1 g L^{-1}; $t = 420$ min).

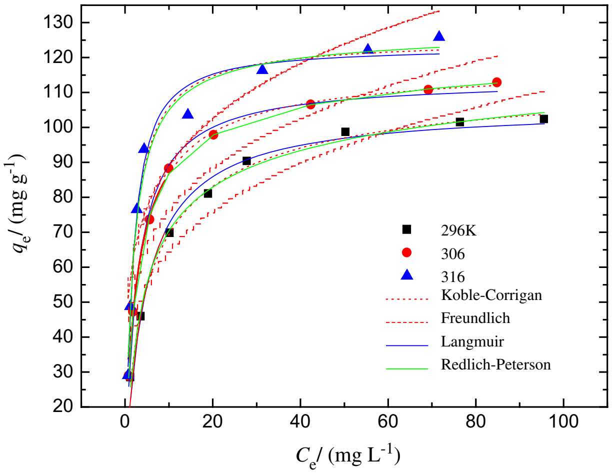

Fig. 9. Langmuir, Freundlich, Redlich–Peterson and Koble–Corrigan Isotherms for adsorption of MG on lotus leaf ($T = 296$, 306, and 316 K; $C_0 = 30$–200 mg L^{-1}; adsorbent concentration = 1 g L^{-1}; $t = 420$ min).

Table 1
Langmuir, Freundlich, Koble–Corrigan and Redlich–Peterson constants for the adsorption of MG onto lotus leaf

Model	296	306	316
Langmuir			
q_m(mg g^{-1})	105.9 ± 2.3	113.8 ± 1.4	125.3 ± 2.8
K_L(L mg^{-1})	0.214 ± 0.024	0.362 ± 0.024	0.541 ± 0.057
R^2	0.985	0.994	0.984
Freundlich			
K_F	37.0 ± 4.3	46.4 ± 5.5	55.3 ± 6.9
$1/n$	0.239 ± 0.031	0.214 ± 0.033	0.205 ± 0.037
R^2	0.984	0.971	0.869
Koble-Corrigan			
A_K	30.5 ± 1.9	46.2 ± 1.3	65.1 ± 7.8
B_K	0.261 ± 0.041	0.388 ± 0.011	0.529 ± 0.064
M	0.748 ± 0.046	0.843 ± 0.026	1.111 ± 0.152
R^2	0.997	0.999	0.985
Redlich–Peterson			
A	31.8 ± 4.5	50.1 ± 2.2	70.6 ± 13.0
B	0.422 ± 0.102	0.530 ± 0.038	0.589 ± 0.192
g	0.92 ± 0.024	0.954 ± 0.007	0.988 ± 0.039
R^2	0.994	0.999	0.984

experimental sorption data than Freundlich isotherm.

The comparison of adsorption capacities of MG onto various adsorbents [9,13–18,33–36] is listed in Table 2. The data show that the lotus leaf used in this study had a relatively large adsorption capacity of MG compared with some data obtained from the published literature. Lotus leaf is not only an excellent adsorbent for MG but also very cost-effective. Compared with the activated carbon, one of the most popular commercial adsorbents used nowadays, lotus leaf is a waste material from agricultural byproduct which is even cheaper. The results indicated that the natural lotus leaf can be considered a promising adsorbent for the removal of MG from aqueous solutions.

Table 2
Comparison of adsorption capacities of MG onto various adsorbents

q_m (mg g^{-1})	Adsorbent	References
178.6	Bentonite	[9]
263.58	Activated carbon prepared from bamboo	[13]
27.78	Activated carbon prepared from the epicarp of Ricinus communis	[14]
4.35	Neem sawdust	[15]
62.71	Rattan sawdust	[16]
78.57	Clayey soil	[17]
48.48	Palm flower activated carbon	[33]
76.92	Activated carbon derived from rice husks	[34]
4.88	Sugarcane dust	[35]
47.9	Mango seed husks	[18]
84.03	Treated ginger waste	[36]
125.3	Lotus leaf	This study

4.8. Kinetic studies

The adsorption kinetics of MG adsorbed on lotus leaf was study the effect of contact time, temperature and initial MG concentration on adsorption. In this investigation, three kinetic models, pseudo-first order, pseudo-second order and intraparticle diffusion models were tested to get the related parameters and adsorption mechanism at different initial concentration and temperature. The kinetic models for MG adsorption are displayed in Figs. 10–14 and the kinetic parameters are presented in Table 3.

Fig. 10 shows a plot of nonlinear form of pseudo-first-order model under different concentration. The values of k_1 and q_{cal} were obtained from the plot of nonlinear form. This model does not give theoretical q_e values that agree with experimental q_e values. The non-linear plots of q_t versus t at different initial

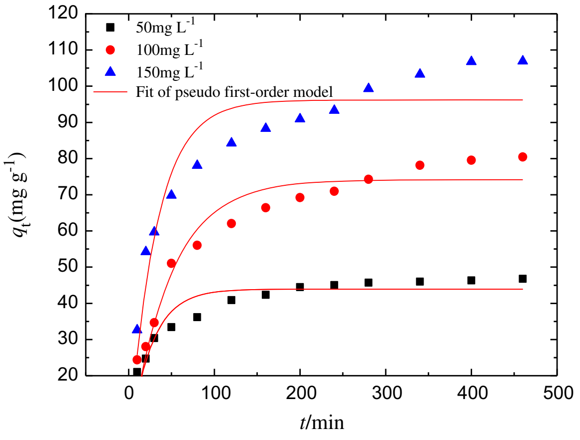

Fig. 10. The pseudo-first-order kinetic plot for the adsorption of MG onto lotus Leaf at different initial dye concentrations ($C_0 = 50{,}100$ and $150\,\mathrm{mg\,L^{-1}}$; $T = 298\,\mathrm{K}$; adsorbent concentration $= 1\,\mathrm{g\,L^{-1}}$; initial pH 4.5).

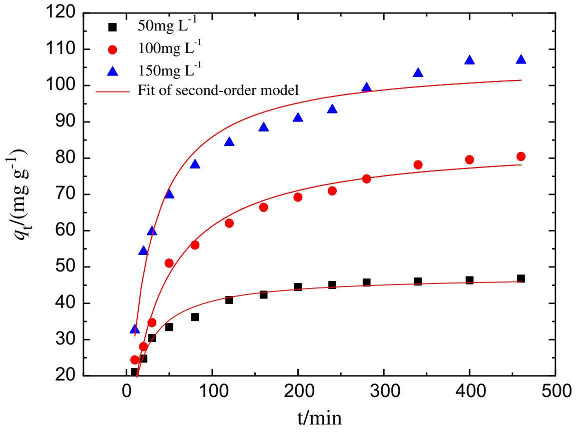

Fig. 11. The pseudo-second-order kinetic plot for the adsorption of MG onto lotus leaf at different initial dye concentrations ($C_0 = 50$, 100 and $150\,\mathrm{mg\,L^{-1}}$; $T = 298\,\mathrm{K}$; adsorbent concentration $= 1\,\mathrm{g\,L^{-1}}$; initial pH 4.5).

concentrations of dye evidence that the pseudo-first-order equation does not fit well for the process of dye adsorption.

Figs. 11 and 12 show the nonlinear plot of the pseudo-second-order model, the correlation coefficients obtained by pseudo-second-order kinetics at different concentrations and temperatures were all above 0.95. Moreover, it can be seen from the Table 3 that the theoretical values of q_e were close to the experimental uptake values. It is also observed from Table 3 that the initial rate of adsorption increases with increasing of solution temperature, which may be due to the increase in driving force at higher temperature. The adsorption capacity q_e in this research increased from 47.67 to $106.85\,\mathrm{mg\,g^{-1}}$ as the initial concentration of MG increased from 50 to $150\,\mathrm{mg\,L^{-1}}$. The adsorption

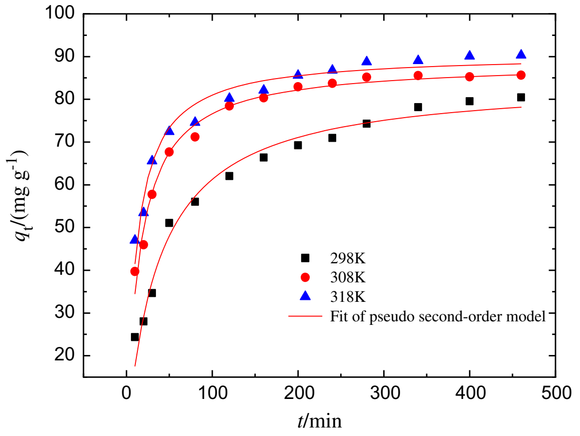

Fig. 12. The pseudo-second-order kinetic plot for the adsorption of MG onto lotus leaf at different temperatures ($T = 298$, 308, and 318 K; adsorbent concentration $= 1\,\mathrm{g\,L^{-1}}$; initial pH 4.5).

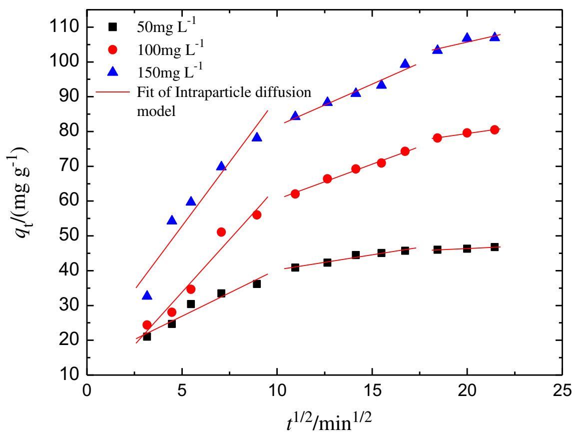

Fig. 13. The intraparticle diffusion model plot for the adsorption of MG onto lotus leaf at different initial dye concentrations ($C_0 = 50{,}100$ and $150\,\mathrm{mg\,L^{-1}}$; $T = 298\,\mathrm{K}$; adsorbent concentration $= 1\,\mathrm{g\,L^{-1}}$; initial pH 4.5).

capacity q_e increased from 84.63 to $90.57\,\mathrm{mg\,g^{-1}}$ as the temperature increased from 298 to 318 K. It is obvious from the result that the adsorption kinetics of MG onto lotus leaf obeyed the pseudo-second-order kinetic model.

The intraparticle diffusion model can also be used to analyze the kinetic data. Figs. 13 and 14 show the plot of q_e against $t^{1/2}$, the values of C and k_{ti} were obtained from the intercept and slope. The results showed that the plots are not linear and can be divided into a few linear regions, which indicate that there are more than one adsorption steps taking place [37]. The stage 1 is the fastest; it should be attributed to external surface adsorption associated with the boundary layer diffusion. The second portion is the

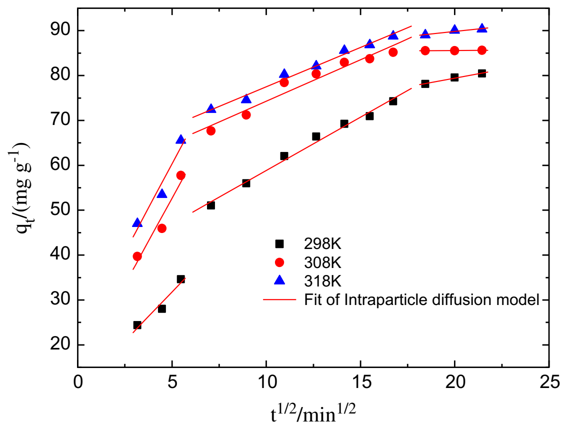

Fig. 14. The intraparticle diffusion model plot for the adsorption of MG onto lotus leaf at different temperatures ($T = 298$, 308, and 318 K; adsorbent concentration = 1 g L^{-1}; initial pH 4.5).

gradual adsorption stage, the slope of the line becomes smaller, where intra-particle diffusion rate is rate-controlling. The third linearity is attributed to the equilibrium stage [38]. However, none of the lines pass through the origin, demonstrating that intraparticle diffusion is not the only rate controlling step but also have some other mechanisms in the whole adsorption process, such as some degree of boundary layer control [39].

In summary, the pseudo-second-order equation is the best one in describing the adsorption kinetics of MG on lotus leaf.

4.9. Thermodynamic properties

The thermodynamic properties were obtained by the adsorption of MG at the temperature of 296 K, 306 K and 316 K. The parameters can evaluate the orientation and feasibility of the physiochemical adsorptive reaction [40]. Three thermodynamic parameters include standard enthalpy (ΔH), standard entropy (ΔS), and standard free energy (ΔG). The parameters can be computed by the following equation:

$$\Delta G = -RT \ln K = \Delta H - T\Delta S \tag{12}$$

$$\ln K = \frac{\Delta S}{R} - \frac{\Delta H}{RT} \tag{13}$$

where K (L mol^{-1}) is Langmuir constant, R is the universal gas constant (8.314 J mol^{-1} K^{-1}), T(K) is the absolute solution temperature, a plot of ΔG vs. T

Table 3
The pseudo-first-order, pseudo-second-order and intraparticle diffusion kinetic parameters for the adsorption of MG onto lotus leaf

Model/C_0/T	50 mg L^{-1}	100 mg L^{-1}	150 mg L^{-1}	298 K	308 K	318 K
Pseudo first-order						
k_1 (L min^{-1})	0.0391	0.0210	0.0311	0.0210	0.0423	0.0543
q_{cal} (mg g^{-1})	43.93	74.15	96.18	74.16	82.23	84.82
R	0.8592	0.9322	0.8774	0.9322	0.9077	0.8371
Pseudo second-order						
$k_2 \times 10^4$	12	3.1	3.8	3.1	7.2	9.3
q_{exp} (mg g^{-1})	46	80	106	80	85	90
q_{cal} (mg g^{-1})	47.67	84.64	106.85	84.63	88.65	90.57
R	0.9675	0.9791	0.9653	0.9791	0.9825	0.9646
Intraparticle diffusion						
k_{t1}	2.68	6.06	7.35	4.35	7.64	7.85
C_1	13.49	3.45	16.04	9.98	14.41	21.02
R	0.9706	0.9751	0.9569	0.9711	0.9683	0.9688
k_{t2}	0.86	2.01	2.41	2.37	1.84	1.75
C_2	31.59	40.33	57.37	35.07	55.77	59.96
R	0.9797	0.9938	0.9791	0.9942	0.9740	0.9925
k_{t3}	0.25	0.77	1.22	0.77	0.026	0.44
C_3	41.23	63.93	81.09	63.93	85.04	80.95
R	0.9920	0.9945	0.8917	0.9945	0.8549	0.9520

should be a straight line, ΔH and ΔS values can be calculated from the slope and intercept of the plot.

The values of ΔG for MG were −10.73, −12.43, and −13.89 kJ mol^{-1} at 296, 306, and 316 K, respectively. The value of ΔH and ΔS for MG was 35.95 kJ mol^{-1} and 157 J mol^{-1}K^{-1}, respectively. The negative ΔG values indicate that the adsorption process is thermodynamically feasible at room temperature and the value of ΔG was found to decrease in the temperature increasing from 296 to 316 K, indicating that the adsorption process of MG on lotus leaf become more favorable at higher temperatures [41]. The positive value of ΔH implies the endothermic nature for the adsorption process. The positive values of ΔS suggest increased randomness at the solid/solution interface and significant changes occur on the surface of the lotus leaf through the dyes adsorption, since the MG species adsorbed on lotus leaf leads to a decrease in the number of the water molecules."

5. Conclusions

In this research, lotus leaf was used as an adsorbent for the removal of MG from aqueous solutions. The Koble–Corrigan, Redlich–Peterson, and Langmuir isotherm models exhibited a better fit to the MG adsorption equilibrium data. The maximum monolayer adsorption capacity of lotus leaf was found to be 125.3 mg g^{-1} at 316 K. The adsorption kinetics follows the pseudo-second-order kinetic model and the intraparticle diffusion was not the sole rate-controlling factor. The adsorption processes were spontaneous and endothermic in nature. The present study suggests that natural lotus leaf can be used as an effective and inexpensive adsorbent for the adsorption of MG from aqueous solutions.

Symbols

A — Redlich–Peterson parameter
A_K — Koble–Corrigan parameter
B — Redlich–Peterson parameter
B_K — Koble–Corrigan parameter
C — intercept
C_0 — initial equilibrium concentration of MG, mg L^{-1}
C_e — equilibrium concentration of MG, mg L^{-1}
K_L — Langmuir constant, L mg^{-1}
K_F — Freundlich constant, mg g^{-1} (L mg^{-1})$^{1/n}$
k_1 — rate constant of the pseudo-first-order sorption, min^{-1}
k_2 — rate constant of the pseudo-second-order sorption, g mg^{-1} min^{-1}
k_t — intraparticle diffusion rate constant, mg g^{-1} min$^{-1/2}$
K — Langmuir constant, L mol^{-1}
$1/n$ — Freundlich constant
m — mass of dry adsorbent, g
M — Koble–Corrigan parameter
q_e — adsorption capacity per unit weight of adsorbent at equilibrium, mg g^{-1}
q_{cal} — calculated value of q_e
q_{exp} — experimental value of q_e
q_m — monolayer biosorption capacity per weight of adsorbent, mg g^{-1}
q_t — adsorption capacity per unit weight of adsorbent at time t, mg g^{-1}
R^2 — correlation coefficient
R — universal gas constant, 8.314J mol^{-1} K^{-1}
t — time, min
T — absolute solution temperature, K
g — Redlich–Peterson parameter
V — volume of solution, L
ΔH — standard enthalpy, kJ mol^{-1}
ΔS — standard entropy, J mol^{-1}K^{-1}
ΔG — standard free energy, kJ mol^{-1}
$R\%$ — adsorption removal of MG

References

[1] H. Chen, J. Zhao, G. Dai, Silkworm exuviae-A new non-conventional and low-cost adsorbent for removal of methylene blue from aqueous solutions, J. Hazard. Mater. 186 (2011) 1320–1327.

[2] V.K. Gupta, Suhas, Application of low-cost adsorbents for dye removal-A review, J. Environ. Manage. 90 (2009) 2313–2342.

[3] J.X. Lina, S.L. Zhana, M.H. Fanga, X.Q. Qian, H. Yang, Adsorption of basic dye from aqueous solution onto fly ash, J. Environ. Manage. 87 (2008) 193–200.

[4] A. Khaled, A. El Nemr, A. El-Sikaily, O. Abdelwaha, Treatment of artificial textile dye effluent containing Direct Yellow 12 by orange peel carbon, Desalination 238 (2009) 210–232.

[5] M. Rafatullah, O. Sulaiman, R. Hashim, A. Ahmad, Adsorption of methylene blue on low-cost adsorbents: A review, J. Hazard. Mater. 177 (2010) 70–80.

[6] C.-H. Weng, Y.-T. Lin, T.-W. Tzeng, Removal of methylene blue from aqueous solution by adsorption onto pineapple leaf powder, J. Hazard. Mater. 170 (2009) 417–424.

[7] J. Mao, S.W. Won, K. Vijayaraghavan, Y.-S. Yun, Immobilized citric acid-treated bacterial biosorbents for the removal of cationic pollutants, Chem. Eng. J. 162 (2010) 662–668.

[8] E.-K. Guechi, O. Hamdaoui, Sorption of malachite green from aqueous solution by potato peel: Kinetics and equilibrium modeling using non-linear analysis method, Arab. J. Chem. (2011), doi:10.1016/j.arabjc.2011.05.011.

[9] E. Bulut, M. Özacar, İ. Ayhan Şengil, Adsorption of malachite green onto bentonite: Equilibrium and kinetic studies and process design, Micropor. Mesopor. Mater. 115 (2008) 234–246.

[10] P. Senthil Kumar, S. Ramalingam, C. Senthamarai, M. Niranjanaa, P. Vijayalakshmi, S. Sivanesan, Adsorption of dye from aqueous solution by cashew nut shell: Studies on equilibrium isotherm, kinetics and thermodynamics of interactions, Desalination 261 (2010) 52–60.

[11] T. Akar, I. Tosun, Z. Kaynak, E. Ozkara, O. Yeni, E.N. Sahin, S.T. Akar, An attractive agro-industrial by-product in environmental cleanup: Dye biosorption potential of untreated olive pomace, J. Hazard. Mater. 166 (2009) 1217–1225.

[12] Z. Aksu, S. Tezer, Biosorption of reactive dyes on the green alga Chlorella vulgaris, Process Biochem. 40 (2005) 1347–1361.

[13] B.H. Hameed, M.I. El-Khaiary, Equilibrium, kinetics and mechanism of malachite green adsorption on activated carbon prepared from bamboo by K_2CO_3 activation and subsequent gasification with CO_2, J. Hazard. Mater. 157 (2008) 344–351.

[14] T. Santhi, S. Manonmani, T. Smitha, Removal of malachite green from aqueous solution by activated carbon prepared from the epicarp of Ricinus communis by adsorption, J. Hazard. Mater. 179 (2010) 178–186.

[15] S.D. Khattria, M.K. Singh, Removal of malachite green from dye wastewater using neem sawdust by adsorption, J. Hazard. Mater. 167 (2009) 1089–1094.

[16] B.H. Hameed, M.I. El-Khaiary, Malachite green adsorption by rattan sawdust: Isotherm, kinetic and mechanism modeling, J. Hazard. Mater. 159 (2008) 574–579.

[17] P. Saha, S. Chowdhury, S. Gupta, I. Kumar, Insight into adsorption equilibrium, kinetics and thermodynamics of Malachite green onto clayey soil of Indian origin, Chem. Eng. J. 165 (2010) 874–882.

[18] A.S. Franca, L.S. Oliveira, S.A. Saldanha, P.I.A. Santos, S.S. Salum, Malachite green adsorption by mango (Mangifera indica L.) seed husks: Kinetic, equilibrium and thermodynamic studies, Desalin. Water Treat. 19 (2010) 241–248.

[19] O.S. Hamdaoui, C.M. Fethi, E. Naffrechoux, Sorption of malachite green by a novel sorbent, dead leaves of plane tree: Equilibrium and kinetic modeling, Chem. Eng. J. 143 (2008) 73–84.

[20] R. Han, Y. Wang, Q. Sun, L. Wang, J. Song, X. He, C. Dou, Malachite green adsorption onto natural zeolite and reuse by microwave irradiation, J. Hazard. Mater. 175 (2010) 1056–1061.

[21] X.S. Wang, Y. Zhou, Y. Jiang, C. Sun, The removal of basic dyes from aqueous solutions using agricultural by-products, J. Hazard. Mater. 157 (2008) 374–385.

[22] A. Zümriye, T. Sevilay, Biosorption of reactive dyes on the green alga Chlorella vulgaris, Process Biochem. 40 (2005) 1347–1361.

[23] B.H. Hameed, D.K. Mahmoud, A.L. Ahmad, Equilibrium modeling and kinetic studies on the adsorption of basic dye by a low-cost adsorbent: Coconut (Cocos nucifera) bunch waste, J. Hazard. Mater. 158 (2008) 65–72.

[24] M.F. Elkady, Amal M. Ibrahim, M.M. Abd El-Latif, Assessment of the adsorption kinetics, equilibrium and thermodynamic for the potential removal of reactive red dye using eggshell biocomposite beads, Desalination 278 (2011) 412–423.

[25] H. Zhang, Y. Tang, X. Liu, Z. Ke, X. Su, D. Cai, X. Wang, Y. Liu, Q. Huang, Z. Yu, Improved adsorptive capacity of pine wood decayed by fungi Poria cocos for removal of malachite green from aqueous solutions, Desalination 274 (2011) 97–104.

[26] I.D. Mall, V.C. Srivastava, N.K. Agarwal, Adsorptive removal of Auramine-O: Kinetic and equilibrium study, J. Hazard. Mater. 143 (2007) 386–395.

[27] T. Akar, B. Anilan, A. Gorgulu, S. Tunali Akar, Assessment of cationic dye biosorption characteristics of untreated and non-conventional biomass: Pyracantha coccinea berries, J. Hazard. Mater. 168 (2009) 1302–1309.

[28] X.S. Wang, Invasive Freshwater macrophyte alligator weed: Novel adsorbent for removal of Malachite green from aqueous solution, Water Air Soil Pollut. 206 (2010) 215–223.

[29] P.S. Kumar, S. Ramalingam, C. Senthamarai, M. Niranjanaa, P. Vijayalakshmi, S. Sivanesan, Adsorption of dye from aqueous solution by cashew nut shell: studies on equilibrium isotherm, kinetics and thermodynamics of interactions, Desalination 261 (2010) 52–60.

[30] N.S. Maurya, A.K. Mittal, P. Cornel, E. Rother, Biosorption of dyes using dead macro fungi: Effect of dye structure, ionic strength and pH, Bioresour Technol. 97 (2006) 512–521.

[31] W.-T. Tsaia, H.-R. Chen, Removal of malachite green from aqueous solution using low-cost chlorella-based biomass, J. Hazard. Mater. 175 (2010) 844–849.

[32] Y.S. Al-Degs, M.I. El-Barghouthi, A.H. El-Sheikh, G.M. Walker, Effect of solution pH, ionic strength, and temperature on adsorption behavior of reactive dyes on activated carbon, Dyes Pigm. 77 (2008) 16–23.

[33] S. Nethaji, A. Sivasamy, G. Thennarasu, S. Saravanan, Adsorption of Malachite Green dye onto activated carbon derived from Borassus aethiopum flower biomass, J. Hazard. Mater. 181 (2010) 271–280.

[34] I.A. Rahman, B. Saad, S. Shaidan, E.S. Sya Rizal, Adsorption characteristics of malachite green on activated carbon derived from rice husks produced by chemical-thermal process, Bioresour. Technol. 96 (2005) 1578–1583.

[35] S.D. Khattri, M.K. Singh, Colour removal from dye wastewater using sugar cane dust as an adsorbent, Adsorpt. Sci. Technol. 17 (1999) 269–282.

[36] R. Ahmad, R. Kumar, Adsorption studies of hazardous malachite green onto treated ginger waste, J. Environ. Manage. 91 (2010) 1032–1038.

[37] E. Bulut, M. Özacar, İ.A. Şengil, Equilibrium and kinetic data and process design for adsorption of Congo Red onto bentonite, J. Hazard. Mater. 154 (2008) 613–622.

[38] L. Abramian, H. El-Rassy, Adsorption kinetics and thermodynamics of azo-dye Orange II onto highly porous titania aerogel, Chem. Eng. J. 150 (2009) 403–410.

[39] N.M. Mahmoodi, B. Hayati, M. Arami, C. Lan, Adsorption of textile dyes on pine cone from colored wastewater: Kinetic, equilibrium and thermodynamic studies, Desalination 268 (2011) 117–125.

[40] M.A. Ahmad, N.K. Rahman, Equilibrium, kinetics and thermodynamic of Remazol Brilliant Orange 3R dye adsorption on coffee husk-based activated carbon, Chem. Eng. J. 170 (2011) 154–161.

[41] G. Kiani, M. Dostali, A. Rostami, A. li, R. Khataee, Adsorption studies on the removal of achite Green from aqueous solutions onto halloysite nanotubes, Appl. Clay Sci. 54 (2011) 34–39.